

Influences of Initiators and Cosurfactants on Microemulsion Polymerization of Vinyltoluene

J. SANTHANALAKSHMI* and K. ANANDHI

Department of Physical Chemistry, University of Madras, A. C. College, Guindy Campus, Madras-600 025, India

SYNOPSIS

Influences of various cosurfactants (CS) (*n*-alcohols and bifunctional alcohols) and initiators (hydrophilic potassiumperoxodisulphate; ammoniumperoxodisulphate and hydrophobic azobisisobutyronitrile; benzoylperoxide) on the polymerization of vinyltoluene–sodium dodecylsulphate–water–CS microemulsions (oil/water μ Es) are studied with respect to the rates of polymerization, molecular weight of polymer, number, and size of polymer particles and energy of activation (E_a). Laser Raman spectroscopy and dilatometry are employed to study the kinetics. Smith Ewart Case II hypothesis seems to be followed in the vinyltoluene μ E polymerization. Stable polymer microlatexes with high molecular weights ($>10^6$) are obtained and particle sizes are found to lie within 10–50 nm as observed from the transmission electron microscopy (TEM) photographs. E_a values varied with different cosurfactants and were found to be comparable with other monomers. Studies of the effects of pH, salt (Na_2SO_4), and inhibitor (hydroquinone) on the microemulsion polymerization showed that optimum pH = 7.0. Higher rates were seen in the absence of salt, and chain transfers to inhibitors take place. © 1996 John Wiley & Sons, Inc.

INTRODUCTION

Microemulsions (μ Es) are multicomponent fluids that consist of an oil, water, surfactant and sometimes cosurfactants (CS), and exhibit microheterogeneity, isotropy, thermodynamic stability, and transparency.^{1–5} One of the most recent applications of the microemulsions μ Es is their utility as media for compartmentalized reactions that are feasible in the microdroplets of μ Es.^{6–8} Several researchers have studied the polymerizations of vinyl monomers in oil/water ionic μ Es with *n*-alkanols and carbitols and without cosurfactants.^{9–27} The polymer particles are of the order 10–50 nm in diameter. Among the numerous cosurfactants used, concern over the cosurfactants that act as destabilizers for latex particles (which is based on their relative hydrophilicity and hydrophobicity) has been put forth by other investigators.^{12,26,27} In the case of polystyrene microlatex formation, butyl cellosolve, when used as a cosurfactant, seems to impart greater stability to the

μ E system.²⁷ Due to the differences in the equilibrium partitioning of an alcohol between different phases, the stability of the μ E during polymerization may vary depending on the nature of the cosurfactant used.

Regarding aromatic vinyl monomers, styrene emulsion^{28–30} and μ E^{14–17} polymerizations have been extensively investigated while there are only few reports regarding the alkyl-substituted styrenes in emulsion polymerization.^{31,32} Alkyl ring substitution renders greater resonance stability of the radicals formed during the propagation steps and hence a lower rate of polymerization is expected. However, reports on such monomers in μ E medium are nearly nil in literature. Vinyltoluene (VT, *p*-methyl styrene) can be microemulsified and polymerized using conventional free radical initiators. The production of microlatexes of polyvinyltoluene is useful in preparing novel polymers, functional polymers, and prepolymers with activated methyl group which can be modified into new and potential polymers.^{31–34} Experimental results regarding the influence of cosurfactants and various types of initiators on VT- μ E polymerization are still lacking. In this study vinyltoluene has been microemulsified in oil/water

* To whom correspondence should be addressed.

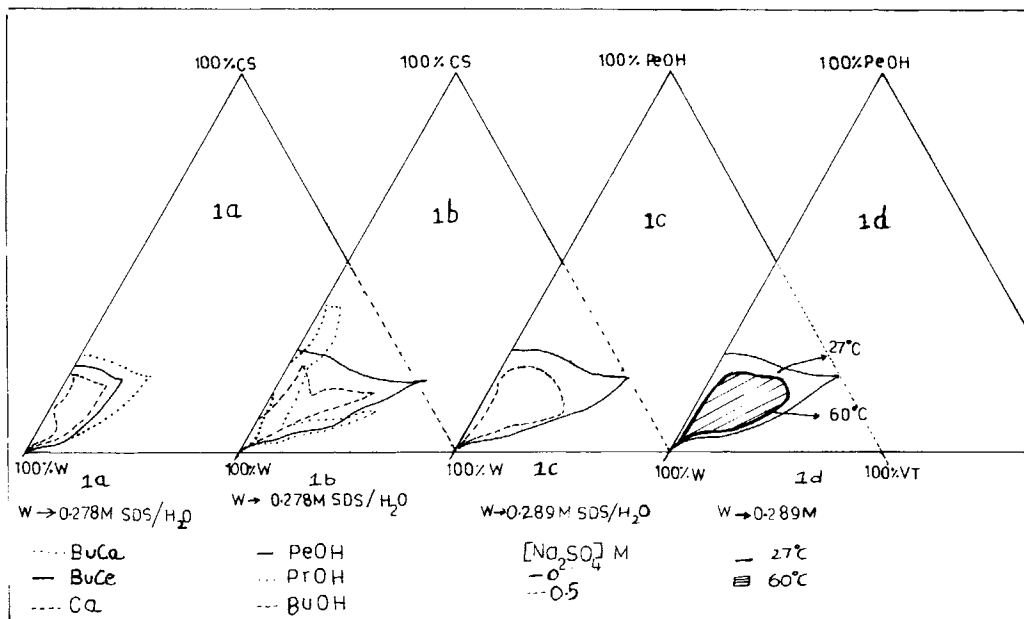


Figure 1 Effect of cosurfactants (a, b), sodium sulfate (c) and temperature (d) on the pseudoternary phase diagrams for oil/water vinyltoluene μ Es. $W = \text{SDS}/\text{H}_2\text{O}$: (a, b) $[\text{SDS}] = 0.278\text{M}$; (c, d) $[\text{SDS}] = 0.289\text{M}$.

μ Es using sodium dodecylsulphate (SDS) as the stabilizer, and polymerized utilizing potassium-peroxodisulphate (KPS, $\text{K}_2\text{S}_2\text{O}_8$), ammoniumperoxodisulphate (APS, $(\text{NH}_4)_2\text{S}_2\text{O}_8$) and azobisisobutyronitrile (AIBN) and benzoyl peroxide (BZ_2O_2) as free radical initiators, each of the pair representing the class of hydrophilic and hydrophobic initi-

ators, respectively. Since oil/water VT-SDS-water-cosurfactant μ Es have been used for the purpose of polymerization, when hydrophilic initiators are present the particle nucleation occurs via the infusion of the primary radicals across the interface; and in the presence of hydrophobic initiators, the polymerization reactions would be initiated in the dis-

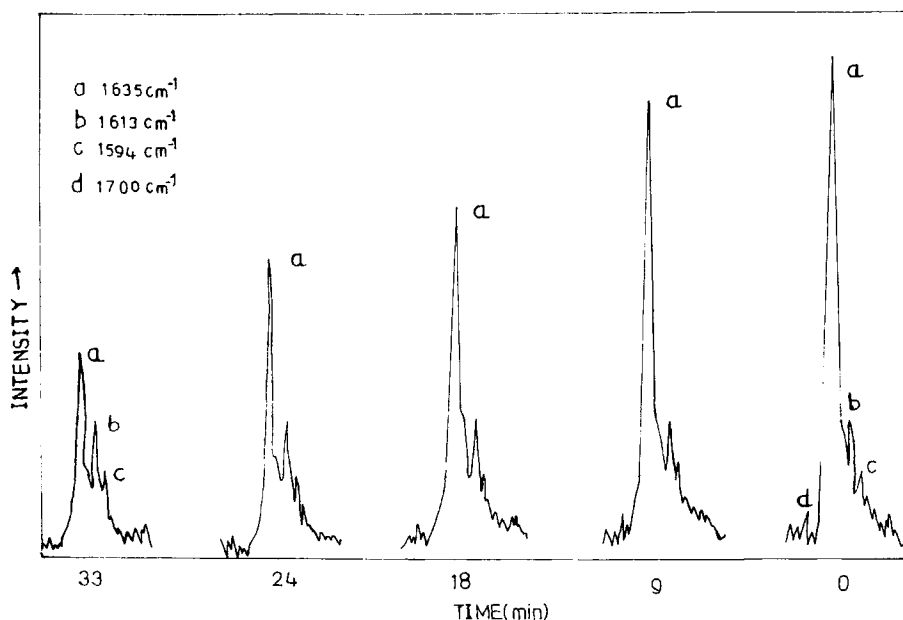


Figure 2 Typical LRS spectra of vinyltoluene μ E polymerization at 70°C in presence of KPS.

Table I Oxygen Effect on R_{pi} , I_p , and Final % Conversion at 70°C ([SDS] = 0.278M; [VT] = 0.5M)

[Initiator] (mM)		R_{pi} [mol/(L s) $\times 10^{-4}$]	I_p (min)	Final % Conversions
[KPS] = 1.00	O ₂	6.27	10	70.00
	N ₂	6.30	4	91.50
[AIBN] = 3.13	O ₂	9.97	17	79.00
	N ₂	10.00	8	97.00

persed phase, resembling a miniaturized bulk polymerization. Hence, studies on the overall rate of polymerization and related kinetic parameter dependences on different types of initiators and co-surfactants, and with respect to variation in surfactant, monomer, and initiator concentrations, would be interesting and useful in establishing a correlation with others of its kind. This report presents investigations on the same. Laser raman spectroscopy (LRS) and dilatometry are used to evaluate the kinetics. Transmission electron microscopy (TEM) and viscosity average molecular weight (\bar{M}_v) are used to characterize the size of the final microlatex and molecular weight of the polymer, respectively. Activation energy of polymerization (E_a) and the co-surfactant influences on the same have also been studied. Additionally, the effects of pH, salt (Na₂SO₄), and inhibitor (hydroquinone, HQ) on the kinetic parameters are also evaluated.

EXPERIMENTAL

Materials

VT, a product of Fluka (Bombay, India), was vacuum-distilled under reduced pressure to remove the inhibitor and stored at -5°C until further use. SDS (AR grade of SD Fine, Bombay, India) was purified by adopting an earlier reported procedure.³⁵ The alcohols, *n*-propanol (*n*-PrOH), *n*-butanol (*n*-BuOH), *n*-pentanol (*n*-PeOH), butylcarbitol [BuCa, 2-(2-butoxyethoxy)ethanol], carbitol [Ca, 2-(2-ethoxyethoxy)ethanol], and butylcellosolve (BuCe, 2-butoxyethanol) were obtained from SD Fine, AR grade, and were used as such. AIBN, BZ₂O₂, APS, and KPS were from Fluka/Aldrich and purified wherever necessary. Toluene from Fischer Scientific (Madras, India) was redistilled and used. Distilled water was used for all experiments.

Methods

The oil/water μE formulations were made by titrating a mixture of VT-water-SDS with PeOH until the

turbidity disappeared. The phase boundaries of the μE region (L_1) were checked by preparing μEs with compositions below and above the required composition and storing the same for a week's time, then visually testing their stability. All μEs were sealed and thermostated during and after formulations. The phase boundaries at 60°C were determined by the addition of methyl ester of HQ to inhibit polymerization.

Polymerization kinetics using LRS were carried out by the addition of the initiator to the μEs ; 5 cm³ of the solution was loaded to the polished quartz sample tube which was degassed under several freeze-and-thaw cycles and carefully sealed under vacuum. The sample tube was then mounted into the sample holder of the Raman Spectrometer. The required temperature of $\pm 1^\circ\text{C}$ was controlled by means of a tight-fitting, heated metal block with holes for the incident and scattered light.

The LRS spectra were obtained with a Cary Model 82 Laser Raman Spectrometer fitted with three sophisticated Czerny Littrow grating monochromators. The laser source utilized was Coherent Innova-70 Argon Laser (4880 Å). The voltage at the sample tube was 800 V. This arrangement allowed simultaneous measurement of all Raman bands within the 1300 cm⁻¹ range with 1.5 cm⁻¹ resolution and with a good signal/noise ratio. Error correction was -10 cm⁻¹. The digital signals were processed and peaks were obtained from an HP 9836 computer interfaced to the spectrometer.

The dilatometer was a double-walled reaction vessel through which thermostated water was circulated; it contained a 40-cm-long capillary (i.d. = 1 mm) and a provision for nitrogen purging. The height variations of the liquid in the capillary column were monitored for kinetics. The dilatometer was precalibrated by comparing the changes in the capillary height with conversion curves obtained by the gravimetric method. The slopes of the conversion versus time plots were used to determine rate of polymerization (R_p). Some of the polymerization reactions were carried out in the presence of oxygen to study the effect of oxygen on the kinetics under similar experimental conditions.

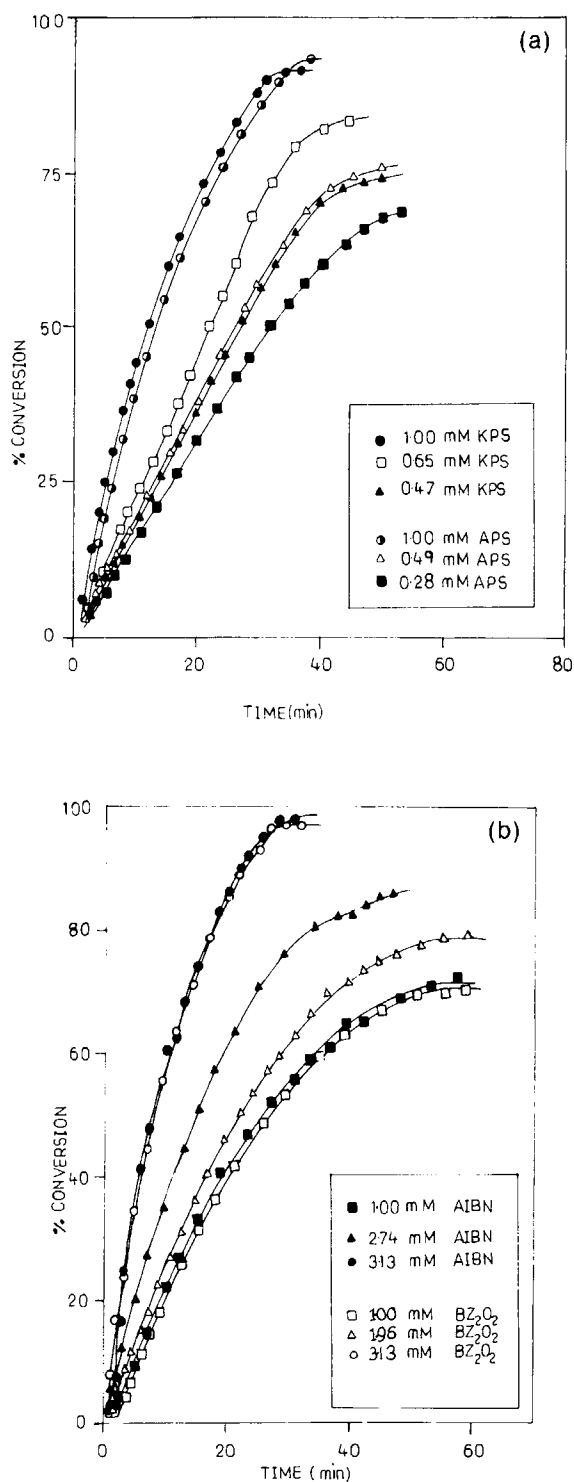


Figure 3 (A) Conversion versus time curves for VT polymerization using various concentrations of KPS [(●) 1.00; (□) 0.65; (▲) 0.47] and APS [(●) 1.00; (△) 0.49; (■) 0.28 mM at 70°C]. [SDS] = 0.278M; [VT] = 0.51M. (B) Conversion versus time curves for VT polymerization using various concentrations of AIBN [(■) 1.00; (▲) 2.74; (●) 3.13] and BZ₂O₂ [(□) 1.00; (△) 1.96; (○) 3.13 mM at 70°C]. [SDS] = 0.278M; [VT] = 0.51M.

Salt effect on R_p was studied using sodium sulphate in the $7 \times 10^{-4}M$ to $3 \times 10^{-2}M$ range. The compositions of μE s prepared using the aqueous salt solution varied slightly but were found to be within the μE region of the phase diagram. pH effect on R_p was studied using buffer tablets in the 5.0–10.0 range. Iolar oxygen (IOL, Madras, India) was used to study the effect of oxygen on kinetic parameters.

Particle sizes of polymerized μE latices were determined using a Philips 400 transmission electron microscope adopting the phosphotungstic acid (PTA) negative staining method.⁹ One drop of polymerized latex in μE was added to 2 mL of 2% PTA solution. Then one drop of this solution was put on a Formvar coated copper 400-mesh grid and TEM photos were taken. The particle diameter (D) was measured by the Zeiss MOP-3 Particle Size Analyser.

After polymerization, the polymerized μE latices were precipitated in a large quantity of methanol. The polymer was washed well with warm water and methanol to remove SDS adhering to the polymers, and dried *in vacuo* at 45°C. \bar{M}_v of the polymer were determined from the relative viscosity coefficient measurements on the dilute polymer toluene solutions at 30°C using a Ubbelohde dilution viscometer, adopting the one-point method of Maron.³⁶ The Mark-Houwink constant values (K and α) were taken as 8.86×10^{-3} mL/g K and 0.74, respectively.³⁷ The viscosity average degree of polymerization (\bar{X}_v) was calculated from \bar{M}_v/M where M is the monomer molecular weight.

RESULTS AND DISCUSSION

Pseudoternary phase diagrams of oil in water ionic μE s are shown in Figure 1. The effects of salt and CS on the phase boundaries indicate that a constriction of the oil solubilization takes place in the presence of sodium sulfate while the presence of PeOH and BuCa enhance oil solubilization into the μE media. At 60°C the extent of oil solubilization decreases. The LRS variation of C=C peak of the monomer with time of polymerization in the presence of KPS at 70°C may be seen from Figure 2. The measurements correspond to 3-min intervals. An exposure time of 1 s was used with a total of 100 scans. A linear relationship between the monomer concentration in the μE and the net integral area of the peak are observed to be in agreement with earlier reports.^{38,39} Data on % conversions of monomer with time and the initial rates after the induction period (I_p) are derived based on the integrated C=C peak area at 1635 cm^{-1} . The base peaks b, c, and d (Fig.

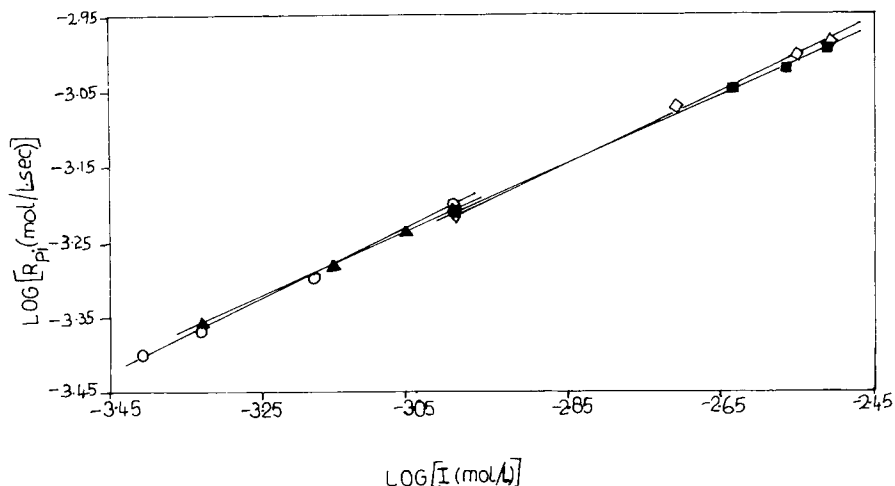


Figure 4 Effect on initiator concentrations on $\log R_{pi}$ of KPS (○), APS (▲), AIBN (■), and BZ_2O_2 (◇) initiated μE polymerizations.

2) do not pertain to the vinyl C=C groups that undergo polymerization. Hence the peak heights of b, c, and d remain invariant with time and thus are

not considered in the area determinations. The rates obtained from LRS measurements are in good agreement with those obtained from dilatometric

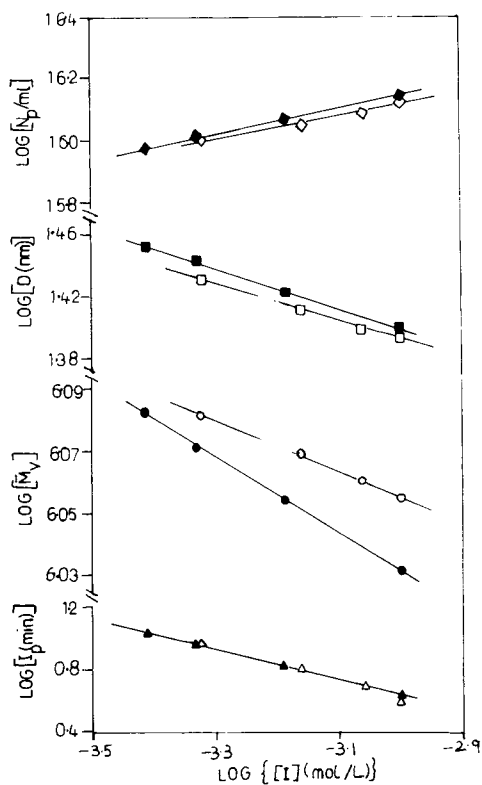


Figure 5 Effect of KPS (filled symbols) and APS on various kinetic parameters and properties of polyvinyltoluene latices.

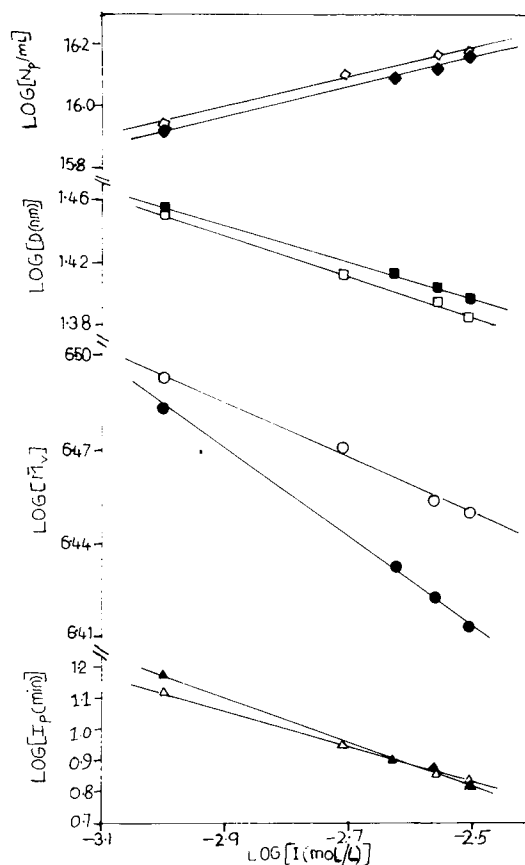


Figure 6 Effect of AIBN (filled symbols) and BZ_2O_2 on various kinetic parameters and properties of polyvinyltoluene latices.

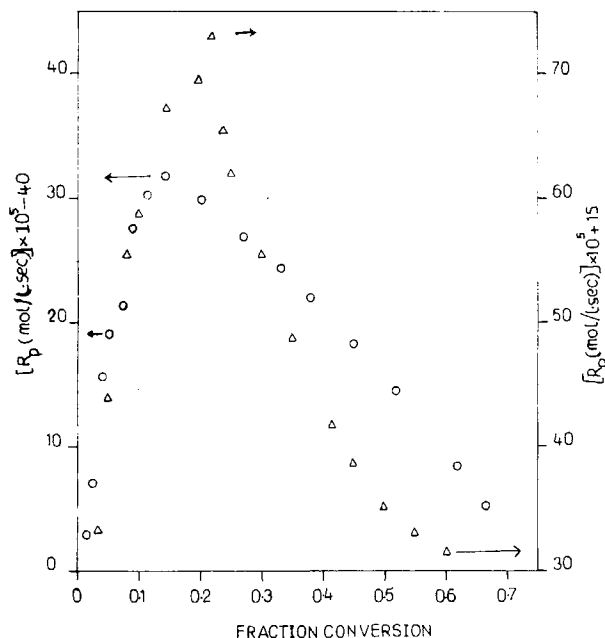


Figure 7 Dependence of R_p on fraction of the monomer polymerized for 0.39 mM KPS (Δ) and 1.0 mM AIBN (O) initiated μE polymerization at 70°C. [VT] = 0.51M; [SDS] = 0.278M.

method. The final polymer microlatexes are translucent and found to be stable for an infinite length of time.

The μE compositions utilized for polymerization fall within the μE boundary regions shown in Figure 1(d). The initial rates of polymerization (R_{pi}) are calculated from the slope of conversion versus time plots at 8% conversion. Table I furnishes the effect of oxygen on R_{pi} , I_p , and final percentage conversions separately for KPS and AIBN systems. Conversion versus time plots in the presence of different concentrations of hydrophilic and hydrophobic initiators ($[I]$) are given in Figures 3(A) and 3(B), respectively. In all cases, increase in $[I]$ causes a decrease in I_p and \bar{M}_v , and an increase in R_{pi} , number of polymer particles (N_p), and final percentage yields. These results are presented in Figures 4, 5, and 6. The R_p -conversion curves are characterized by an increase in rate with conversion, reaching a maximum (R_{pmax}) and followed by a decrease (Fig. 7). R_{pmax} occurs at lower conversions (15–20%) for AIBN and BZ_2O_2 than for KPS and APS systems, which occur around 20–25%, respectively. The monomer concentration variations on $\log R_{pi}$ are shown in Figure 8 for KPS and AIBN systems. In the presence of other initiators, similar trends are seen. The collective dependences of $\log R_{pi}$, $\log \bar{M}_v$, and $\log N_p$ on $\log [I]$ for various initiators are given

in Table II. These values are the slopes of the log-log plots illustrated in Figures 5 and 6. R_{pi} dependences on the exponential powers of the monomer concentration are found to lie within 1.2–1.6. Influence of CS on R_{pi} , I_p , \bar{M}_v , \bar{X}_v , E_a , and D for KPS μEs is presented in Table III. Similar trends are found with other initiators. In the presence of hydrophilic inhibitors (HQ), the inhibition period (*tin*) exhibits a direct function of HQ concentration (Fig. 9). After *tin*, percentage conversion-time curves proceed unaltered. The \bar{M}_v decrease with HQ concentration is seen in Figure 9. Figure 10 gives the Arrhenius plot of VT μE polymerization in the presence of KPS and AIBN. Effects of pH on $\log R_{pi}$ and of salt concentration on R_{pi} , I_p , and \bar{M}_v are given in Figure 11 and Table IV. The sizes of final polymer microlatexes are analyzed by TEM, and typical microphotographs are presented in Figure 12. Variation in \bar{M}_v , \bar{X}_v , and D with changes in monomer weight fractions are presented in Table V. Table VI illustrates the effect of changes in SDS concentration ([SDS]) on R_{pi} , I_p , \bar{M}_v , N_d , \bar{X}_v , D , and final % yield of polymerization.

For a free radical type of initiation, the presence of oxygen increases I_p while R_{pi} values are unaltered. Such effects are due to the quenching of primary radicals, and when the induction period is overcome the rate of polymerization remains the same. Lower yields for KPS than AIBN in O_2 may be attributed to the lesser effect of O_2 on AIBN which produces some N_2 on its decomposition.^{40,41}

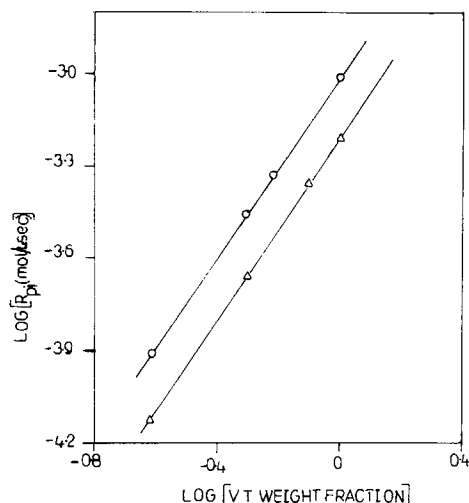


Figure 8 Effect of monomer concentration variations on $\log R_{pi}$ for 1.0 mM KPS (Δ) and 3.13 mM AIBN (O) initiated microemulsion polymerizations at 70°C. [SDS] = 0.278M; VT weight fraction = wt of VT/(VT + Toluene).

Table II Kinetic Parameters for Initiators

Initiator Type	[VT]	$\log [R_p]$	$\log [\bar{M}_v]$	$\log [N_p]$
KPS	1.2	0.49	-0.125	0.37
AIBN	1.5	0.42	-0.151	0.38
BZ ₂ O ₂	1.6	0.48	-0.09	0.39
APS	1.3	0.49	-0.08	0.38

For all initiators, I_p decreases with increase in $[I]$ (Figs. 5 and 6) because of the increase in the number of primary radicals per particle produced by the initiator decompositions. Initiations in aqueous media (KPS and APS) show lower I_p values than the hydrophobic initiations (AIBN and BZ₂O₂). Decomposition rates of hydrophilic initiators are enhanced over hydrophobic initiators in the presence of soap solutions.^{17,42} This results in a higher rate of primary radical generation for the hydrophilic initiations which result in lower I_p values. Similar I_p values are observed for KPS- and APS-initiated systems. I_p values for BZ₂O₂ are lower than AIBN systems due to the partitioning of AIBN into the other μE phases.^{43,44} Regardless of type and concentration of initiator, monomer, surfactant, cosurfactant, or temperature, the reaction rate exhibits two regions: the rate increases with conversion (region I) reaches a maximum (R_{pmax}) and then decreases with conversion (region II). Such behavior has been reported earlier.^{9,10,44} Region I is considered to be the nucleation stage, wherein the number of polymerization loci increases with time. When all the μE droplets have disappeared, either by becoming polymer particles or by diffusion of the monomer to polymer particles, the rate decreases (region II) due to the decrease of monomer concentration in the monomer-swollen polymer particles. The order dependences of $\log R_{pi}$, $\log \bar{M}_v$, and $\log N_p$ on $\log [I]$ are given in Table II. The dependence of R_{pi} on $[I]$ is found to be consistent with the Smith Ewart Case

II hypothesis.^{9,17,45} Similar dependence of R_{pi} on $[I]$ for all initiators indicates that the nucleation process and the radical source for initiation mechanisms are the same in all the initiators.

The final particle sizes are independent of initiators and lie within the range of 10–50 nm. Regarding the sizes of the polymer microlatices: D decreases as $[I]$ increases, since the number of radically activated droplets as well as the termination steps increase with $[I]$. The slight differences observed in the dependency of the initiators with \bar{M}_v might be attributed to the differences in the solubilities and in the times of residence of the free radicals in the micelles containing the polymer particles.^{9,10} The polymer particle number density (N_p) is calculated from the number average diameter of the final latex based on the TEM studies carried out at the end of the polymerization. The dependences of $\log N_p$ with $\log [I]$ also indicate a Smith Ewart Case II type of polymerization to be followed (Table II). In the case of μE droplets, particle nucleations are likely to occur in droplets and the fraction becoming particles is determined by the level of initiators and the radical flux into the droplets.^{9,10} However, the probability of homogeneous nucleations in the aqueous phase is significant due to the large surface area provided by the μE and the hydrophobicity of the monomer. The gel effect as observed in the conventional emulsion polymerization systems^{46,47} is not found here. The reasons could be attributed to the small-sized latex particles; where in the polymer-

Table III Effect of Cosurfactants on R_p , I_p , \bar{M}_v , \bar{X}_v , E_a , and D for VT μE at 70°C ([KPS] 1.0 mM; [SDS] = 0.278M)

CS	R_{pi} [mol/(L s) $\times 10^{-4}$]	I_p (min)	$\bar{M}_v \times 10^6$	\bar{X}_v	E_a (kcal/mol)	D (nm)
<i>n</i> -PrOH	5.08	12	0.67	5674	15.1	23.8
<i>n</i> -BuOH	5.75	7	0.94	7961	18.0	24.5
<i>n</i> -PeOH	6.300	4.1	1.0	8469	19.8	25.0
Ca	6.01	5.5	0.86	7283	17.4	24.2
BuCa	6.28	4.1	1.0	8469	19.8	25.0
BuCe	5.69	9	0.704	5962	16.0	23.5

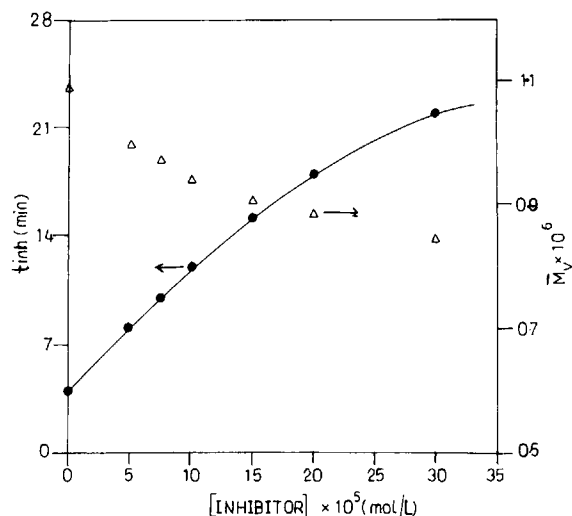


Figure 9 \bar{M}_v (Δ) and t_{inh} (\bullet) with variation in inhibitor concentration. [KPS] = 1.0 mM; [SDS] = 0.278M; [VT] = 0.51M.

ization, nucleations are immediately followed either by chain transfer termination or by desorption of propagating radicals.

Figure 8 and Table V show that when the monomer concentration is decreased in the oil phase, R_{pi} , \bar{M}_v , and D values decrease. The order dependences are similar in the presence of four initiators (Table III). Presence of toluene which is incorporated for monomer dilutions increases the solvent chain transfers⁹ and therefore produces the observed trends in R_{pi} , \bar{M}_v , and D (Table V).

The polymerization reactions conducted in μE medium depend on the surfactant concentration. Here SDS is maintained above the cmc value (cmc = $8.27 \times 10^{-3}M$),^{48,49} so that the number density of the oil-swollen micelles is more than the primary radicals and an efficient droplet nucleation may be effected. Increase in [SDS] increases only the number density of the droplets and exceeds the droplet depletions during polymerization, so that R_{pi} , I_p , and \bar{M}_v are observed to be unaltered. Even though a direct correlation cannot be maintained between the sizes of initial and final oil-swollen SDS micelles, increase in [SDS], i.e., the SDS/oil mole ratio, seems to decrease the droplet volumes (Table VI).

According to the Smith Ewart Case II hypothesis, R_p is directly proportional to the monomer concentration within the growing polymer particle. So the other overall polymer kinetic parameters depend critically on the monomer solubilization into the droplet core, CS partitionings into different phases, stability of the interface, feasibility of the radical transfer across the interface, termination of radicals

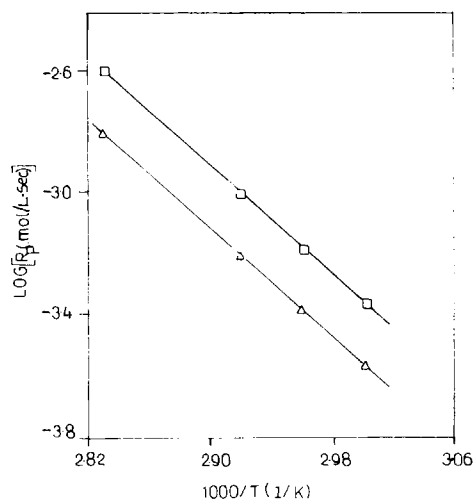


Figure 10 Arrhenius plots for VT μE polymerization initiated by 1.0 mM KPS (Δ) and 3.13 mM AIBN (\square).

through desorption across the interface, etc. These processes are greatly influenced by hydrophilicity and hydrophobicity of the cosurfactants and the solubility of the monomer oil along with the interfacial fluidity, etc.,. In the case of hydrophilic initiators, the cosurfactants partitioned into aqueous phase also act as interfacial radical transfer agents with respect to the droplet monomers. Thus lower I_p values are observed for *n*-PeOH and BuCa cosurfactants due to their effective partitioning across the interface. The $\log R_{pi}$ order dependences on [I] and [VT] concentration are nearly the same in the presence of various types of cosurfactants and are similar to that predicted by the Smith Ewart Case II hypothesis. Sizes of the final polymer microlatices seem to be uninfluenced by the cosurfactants, indicating that the cosurfactants influence only the

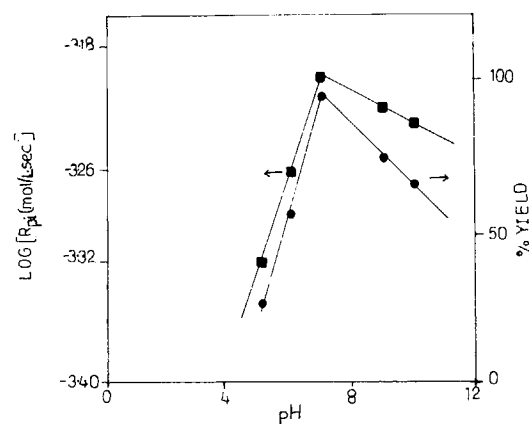


Figure 11 Effect of pH on $\log R_{pi}$ (\blacksquare) and % yield (\bullet); [KPS] = 1.0 mM.

Table IV Effect of Salt on R_{pi} , I_p , \bar{M}_v , and \bar{X}_v on VT μE Polymerization ([SDS] = 0.278M; [VT] = 0.5M; [KPS] 1.0 mM)

[Na ₂ SO ₄] (mM)	I_p (mins)	R_{pi} [mol/(L s) $\times 10^{-5}$]	$\bar{M}_v \times 10^6$	\bar{X}_v
0	4	63.00	1.09	9231
0.7	7	30.20	0.96	8130
6.1	12	19.00	0.86	7283
11.2	18	13.00	0.72	6098
20.0	32	8.10	0.54	4573
30.0	40	4.77	0.43	3642

particle nucleations and radical transfer steps rather than the overall polymerization mechanisms.

\bar{M}_v is found to be different depending on the type of the cosurfactant used (Table III). This indicates that radical chain terminations occur not only by combination/disproportionation steps but also via chain transfers with the cosurfactants. There are reports indicating that cosurfactants act as chain transfer agents.⁵⁰⁻⁵³ Since direct chain transfer con-

stants are not available for various cosurfactants, chain transfer constants between vinyl monomer and some alcohols possessing similar functional groups may be considered. For *n*-PrOH, *n*-BuOH and 1,2-ethanediol, the values are 1.6, 2.0, and 1.4×10^{-4} , respectively.⁵² Thus it is expected that PeOH and BuCa would produce lesser chain transfer producing higher \bar{M}_v . These effects may be considered as the indirect influences of the cosurfactants that

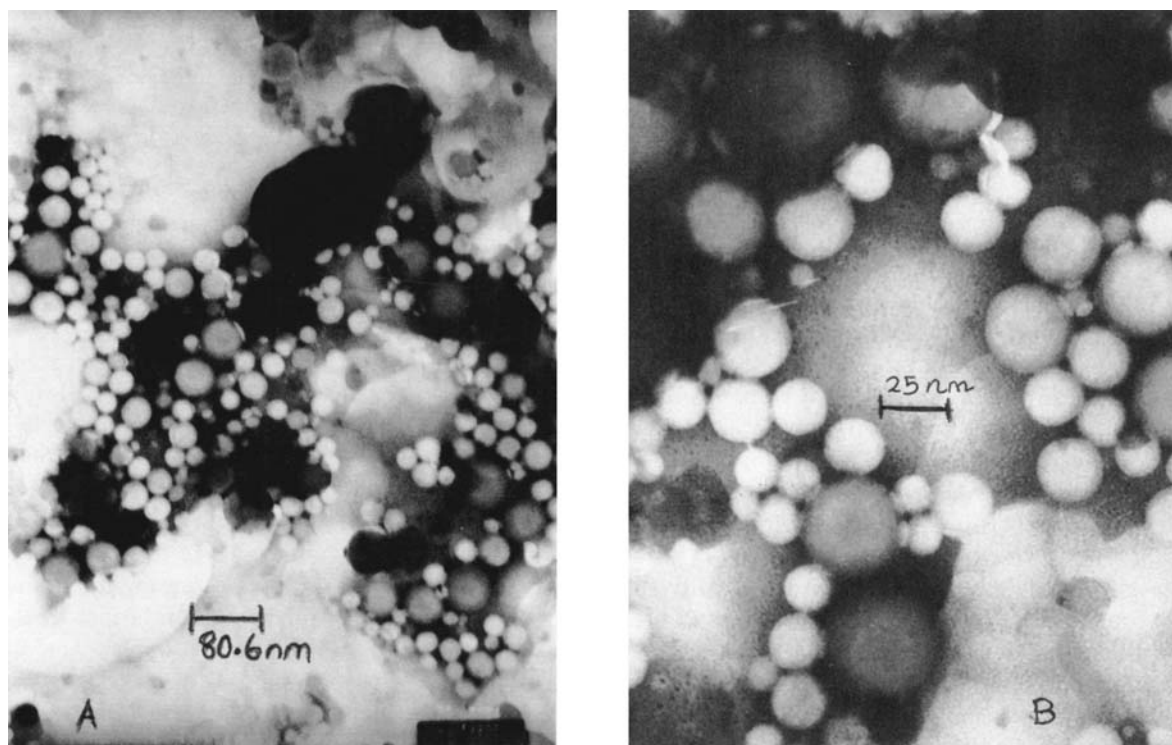


Figure 12 Transmission electron microphotographs of final polymer microlatex prepared by μE polymerization of vinyltoluene at 70°C. [SDS] = 0.278M; (A) 1.0 mM KPS; [VT] = 50% by wt; (B) 3.13 mM AIBN; [VT] = 100% by wt. SCALE BAR FOR 1 CM.

Table V \bar{M}_v , \bar{X}_v , and D for VT μE Polymerization at Various Weight Fractions of VT at 70°C ([SDS] = 0.289M; [KPS] = 0.65 mM)

VT (wt %)	$\bar{M}_v \times 10^6$	\bar{X}_v	D (nm)
KPS			
100	1.10	9316	25.9
80	1.01	8554	24.2
60	0.91	7707	22.9
50	0.83	7929	21.4
AIBN			
100	2.58	21850	26.6
80	2.53	21456	25.9
60	2.46	20833	25.1
50	2.40	20325	24.2

affect the rates of radical initiations and terminations in the particles.

The salt effect is studied in particular to KPS systems using Na_2SO_4 . When the [salt] increases, the process of primary radical transfer between the species in the aqueous phases also increases, shortening the life time of the radicals and consequently increasing the I_p values. The decrease in R_{pi} is due to the decrease in the rate of transfer of initiating primary radicals to the droplets. Appearance of early phase separation may be attributed to the electrolytic effect on μE s. In the presence of excess SO_4^{2-} anions, the fraction of free counterions of the droplets increases which aids the radical desorptions to the aqueous phase. Thus \bar{M}_v decreases.

The decomposition of KPS in aqueous medium has been reported to render the medium slightly acidic.⁵⁴ Hence pH effect is studied for the KPS system. The dispersion medium is acidic and contains more $[\text{H}^+]$ so that the primary radical transfer to H^+ occurs in addition to other species in the aqueous phase.³² This lowers R_{pi} and % yield values and increases I_p . Above pH = 7.0, similar observations are seen. Thus in the presence of H^+ or H^- , the approach of the sulphate radicals to the anionically charged droplet interface is suppressed. These observations make pH = 7.0 the optimum pH for the μE polymerization, which proves that the radical infusion across the interface is the decisive factor for nucleation in the μE droplets.

Increase in hydroquinone concentration ([HQ]) is found to increase the I_p , which may be due to the quenching of the initiator free radicals. Once inhibition is overcome, the initiated polymerization shows unaffected conversion-time dependences. This shows that the reactivity of the monomer re-

mains unaffected due to the HQ addition. On increasing [HQ], \bar{M}_v is found to decrease, indicating chain transfers between the propagating radicals and inhibitor or its radicals formed by its interaction with the initiators.

The R_{pi} values increase with temperature. This may be due to the increase in the number density of the droplets that occurs via temperature-dependent micellar breakdown processes, as well as due to the increase in the radical generation rate processes. As there is a probable concomitant increase in radical termination steps with temperature, \bar{M}_v values show a decrease with increasing temperature. From the Arrhenius plot, the overall activation energy (E_a) of the polymerization has been found to be 20.4 kcal/mol. This value agrees with the E_a of the overall polymerization of vinyl monomers.⁵⁵ E_a is found to be nearly independent of the type of initiator utilized in μE polymerization. On varying the CS, the E_a values are found to be higher for *n*-PeOH and BuCa (Table III). Overall effects of initiation, propagation, and termination steps affect E_a according to the equation $[E_i + (E_p - E_t)]/2$, where E_i , E_p , and E_t are activation energies of initiation, propagation, and termination steps, respectively. On going from PeOH to BuCa-Ca-BuOH-BuCe-ProOH, partitioning across the droplet increases, which results in the lowering of E_i and E_t ; this subsequently decreases the E_a of other cosurfactants.

CONCLUSION

The polyvinyltoluene latex suspensions prepared are found to be stable and lie within the range of 10–50 nm. The molecular weights lie within the $1\text{--}3.5 \times 10^6$ daltons. For both the hydrophilic and hydrophobic initiators, the propagation and termination steps remain unaltered. Even though I_p values for hydrophilic initiators are lower than for hydrophobic initiators, R_{pi} and N_p show similar dependences with all the initiators. Regarding the influence of the cosurfactant, *n*-pentanol seems to impart better stability, higher values of kinetic parameters, and appreciable \bar{M}_v of the polymer microlatices of the vinyltoluene. The μE kinetics resemble the Smith Ewart Case II hypothesis of the emulsion polymerization. The results indicate better rate values of the μE and remain comparable and reasonable to that of vinyl polymerization in spite of the microheterogeneity of the μE s, and are altered in the presence of different cosurfactants.

Table VI R_{pi} , I_p , N_d , \bar{M}_v , \bar{X}_v , D , and Final % Yield for VT μE Polymerization at Various Surfactant Concentrations ([KPS] = 0.65 mM)

[SDS] (M)	R_{pi} [mol/(L s) $\times 10^{-4}$]	I_p (min)	N_d (mL $\times 10^{16}$)	\bar{M}_v ($\times 10^6$)	\bar{X}_v	D (nm)	Final % Yield
0.219	4.98	6.1	1.88	1.12	9485	28.9	83.3
0.249	5.10	6.5	2.143	1.14	9654	27.6	82.7
0.278	5.00	6.6	2.399	1.11	9400	26.2	84.0
0.305	5.04	6.4	2.622	1.13	9570	25.2	84.8

The authors are grateful to UGC, India, for financial help in this work. They also thank IIT, Bombay, for LRS measurements, and CDRI, Lucknow, for TEM results.

REFERENCES

- L. E. Scriven, *Micellization, Solubilization and Microemulsions*, K. L. Mittal, Ed., Plenum Press, New York, 1987, p. 877.
- L. Danielsson and B. Lindman, *Colloids Surf.*, **3**, 391 (1981).
- M. J. Hou, M. Kim, and D. O. Shah, *J. Colloid Interface Sci.*, **123**, 398 (1988).
- W. John and R. Strey, *J. Phys. Chem.*, **92**, 2294 (1988).
- D. Langevin, *Adv. Colloid Interface Sci.*, **34**, 583 (1991).
- G. Gillberg, *Emulsions and Emulsion Technology*, K. J. Lissant, Ed., Dekker, New York, 1986, Part 3, p. 1.
- K. Shinoda and B. Lindman, *Langmuir*, **3**, 135 (1987).
- J. H. Fendler, *Membrane Mimetic Chemistry*, Wiley, New York, 1962.
- M. S. El-Aasser, J. W. Vanderhoff, and J. S. Guo, *J. Polym. Sci., Polym. Chem. Ed.*, **27**, 691 (1989).
- L. M. Gan, C. H. Chew, K. C. Lee, and S. C. Ng, *Polymer*, **34**, 3064 (1993).
- P. L. Kuo, N. J. Turro, C. M. Tseng, M. S. El-Aasser, and J. W. Vanderhoff, *Macromolecules*, **20**, 1216 (1987).
- S. S. Atik and J. K. Thomas, *J. Am. Chem. Soc.*, **103**, 4279 (1983).
- J. S. Guo, M. S. El-Aasser, E. D. Sudol, H. J. Yue, and J. W. Vanderhoff, *J. Colloid Interface Sci.*, **149**, 184 (1992).
- M. Antonietti, W. Bremser, D. Muschenborn, C. Rosenauer, B. Schupp, and M. Schmidt, *Macromolecules*, **24**, 6636 (1991).
- M. Antonietti, S. Lohmann, and C. Van Niel, *Macromolecules*, **25**, 1139 (1992).
- V. H. Perez-Luna, J. E. Puig, V. M. Castano, B. E. Rodriguez, A. K. Murthy, and E. W. Kaler, *Langmuir*, **6**, 1040 (1990).
- J. S. Guo, E. D. Sudol, J. W. Vanderhoff, and M. S. El-Aasser, *J. Polym. Sci., Polym. Chem. Ed.*, **30**, 691 (1992).
- F. Bleger, A. K. Murthy, F. Pla, and E. W. Kaler, *Macromolecules*, **27**, 2559 (1994).
- L. M. Gan, C. H. Chew, K. C. Lee, and S. C. Ng, *Polymer*, **35**, 2659 (1994).
- M. R. Ferrick, J. Murtagh, and J. K. Thomas, *Macromolecules*, **22**, 1515 (1989).
- C. Larpent and T. F. Tadros, *Colloid Polym. Sci.*, **269**, 1171 (1991).
- F. Candau, Z. Zekhnini, and F. Heatley, *Macromolecules*, **19**, 1895 (1986).
- E. Haque and S. J. Qutubuddin, *J. Polym. Sci., Polym. Lett. Ed., Part C*, **26**, 429 (1988).
- F. Candau, Y. S. Leong, G. Pouyet, and S. J. Candau, *Colloid Interface Sci.*, **101**, 167 (1985).
- S. Qutubuddin, C. S. Lin, and Y. Tajuddin, *Polymer*, **35**, 4606 (1994).
- A. Jayakrishnan and D. O. Shah, *J. Polym. Sci., Polym. Lett. Ed.*, **22**, 31 (1984).
- L. M. Gan, C. H. Chew, and S. E. Friberg, *J. Macromol. Sci. Chem.*, **A19**, 739 (1983).
- B. C. Y. Whang, D. H. Napper, M. J. Ballard, and R. G. Gilbert, *J. Chem. Soc. Faraday, Trans. 1*, **78**, 1117 (1982).
- I. A. Maxwell, B. R. Morrison, D. H. Napper, and R. G. Gilbert, *Macromolecules*, **24**, 1629 (1991).
- W. A. Al-Shabib and A. S. Dunn, *Polymer*, **21**, 429 (1980).
- K. P. Paoletti and F. W. Bilmeyer, Jr., *J. Polym. Sci., Part A.*, **2**, 2049 (1964).
- D. C. Blackely, *Emulsion Polymerization*, Applied Science Publishers, Ltd., New York, 1975, p. 418.
- W. T. Ford and T. Balakrishnan, *Macromolecules*, **14**, 284 (1981).
- W. T. Ford and T. Balakrishnan, *J. Org. Chem.*, **48**, 1031 (1983).
- D. C. Blackely and W. P. H. Burger, in *Emulsion Polymerization*, Irija Piirma, and J. K. Gorden, Eds., ACS Symp. Series, No. 24, American Chemical Society, Washington, DC, 1976, p. 162.
- S. H. Maron, *J. Appl. Chem.*, **5**, 282 (1961).
- J. Brandrup and E. H. Immergut, *Polymer Handbook*, 3rd Edn., Wiley, New York, 1975, Chapter IV.
- E. Gulari, K. Mckeigue, and K. Y. S. Ng, *Macromolecules*, **17**, 1822 (1984).
- L. Feng and K. Y. S. Ng, *Macromolecules*, **23**, 1048 (1990).

40. C. H. Bamford, W. G. Barb, A. D. Jenkins, and P. F. Onyan, *The Kinetics of Vinyl Polymerization by Free Radical Mechanisms*, Academic Press, New York, 1958.
41. G. Odian, *Principles of Polymerization*, 2nd Edn, John Wiley and Sons, New York, 1981.
42. A. E. Alexander and D. H. Napper, *Progress in Polymer Science*, Vol. 3, A. D. Jenkins, Ed., Pergamon Press, Oxford, 1971, p. 145.
43. V. Vaskova, V. Juranicova, and J. Barton, *Makromol. Chem.*, **191**, 717 (1990); **193**, 627 (1992).
44. L. A. Rodriguez-Guadarrama, E. Mendizabal, J. E. Puig, and E. W. Kaler, *J. Appl. Polym. Sci.*, **48**, 775 (1993).
45. W. V. Smith and R. H. Ewart, *J. Chem. Phys.*, **16**, 592 (1948).
46. G. T. Russel, R. G. Gilbert, and D. H. Napper, *Macromolecules*, **26**, 3538 (1993).
47. J. Barton and A. Karpatyova, *Makromol. Chem.*, **44**, 693 (1961).
48. A. B. Mandal, S. Ray, and S. P. Moulik, *Ind. J. Chem.*, **19A**, 620 (1980).
49. P. Mukerjee and K. J. Mysels, *Critical Micelle Concentration of Aqueous Surfactant Systems*, Natl. Std. Ref. Data Series, National Bureau of Standards, Washington, DC, 1971.
50. D. Donescu, D. F. Anghel, and M. Balcan, *Die. Angewandte Makromolekulare Chemie.*, **175**, 1 (1990).
51. L. M. Gan, C. H. Chew, I. Lye, L. Ma, and G. Li, *Polymer*, **34**, 3860 (1993).
52. J. Brandrup and E. H. Immergut, *Polymer Handbook*, 3rd Edn., Wiley, New York, 1975, Chapter II.
53. H. I. Tsang, P. L. Johnson, and E. Gulari, *Polymer*, **25**, 1357 (1984).
54. I. M. Kolthoff and E. M. Carr, *J. Am. Chem. Soc.*, **73**, 3055 (1951).
55. P. J. Flory, *Principles of Polymer Chemistry*, Cornell University Press, Ithaca, NY, 1953.

Received March 1, 1995

Accepted June 17, 1995